

Morphological characterization of branched PP under stretching

W. L. Oliani · D. F. Parra · L. F. C. P. Lima ·
A. B. Lugao

Received: 10 February 2011 / Accepted: 15 January 2012 / Published online: 26 January 2012
© Springer-Verlag 2012

Abstract An effective approach to achieve high-melt strength polymer is to add long chain branches onto backbone species using gamma radiation. Grafting and branching result from macroradicals combinations during the irradiation process. Polypropylene films were prepared starting with irradiation process of the pellets with a ^{60}Co source at doses of 5, 12.5, and 20 kGy under acetylene to improve melt strength and drawability. After irradiation, polypropylene films were obtained by compression molding, at 190 °C and pressure of 80 bar, and dive into a water tank at 23 °C, which generally favors the formation of an amorphous phase. The thin films were stretched at 170 °C using a universal testing machine. Film surface morphology and the thermal properties, were analyzed, using atomic force microscopy, scanning electron microscopy and differential scanning calorimetry. We had a different molecular structure that requested the study of their micro and nanostructure. The results showed some evidence of fibrillar structures containing crystallites and gel formation. Fibrils oriented along the stretching direction were observed.

Keywords Stretching · Crosslinking · Polypropylene and gamma radiation

Introduction

Commercial isotactic polypropylene (iPP) has a non-polar molecule and is structured in linear chains as a result of its production via Ziegler–Natta. As a

W. L. Oliani (✉) · D. F. Parra · L. F. C. P. Lima · A. B. Lugao
Nuclear and Energy Research Institute, IPEN-CNEN/SP, Av. Prof. Lineu Prestes,
2242 Cidade Universitária, São Paulo, SP 05508-000, Brazil
e-mail: washoliani@yahoo.com.br

A. B. Lugao
e-mail: ablugao@ipen.br

consequence, iPP has a relatively low melt strength at processing temperatures [1–3]. A long-chain branched polypropylene (PP) until recently was only possible by the radical modification of the linear iPP macromolecules from the polymerization process [4]. Our institute developed the production of branched PP, based on the grafting of long chain branches on PP backbone using acetylene as a crosslink promoter under a gamma radiation process. The resulting grafting reactions occurred on rearrangement of the radicals formed in the polymer. However, if multifunctional monomers were used, the kinetics of crosslinking could be increased and eventually the melted polymer under processing to be excessively elastic with poor drawability [5]. The primary process due to polymer irradiation is the generation of excited species and free radicals arising from the breakdown of chemical bonds. The radicals produced can react, resulting in crosslinking or chain scission [6, 7]. The two mechanisms of chain scission and crosslinking usually occur simultaneously but depending on the radiation dose level one mechanism can become more prominent than another [8]. iPP undergoes crosslinking and extensive main-chain scissions when submitted to irradiation. Particularly in the presence of acetylene, the simultaneous irradiation of PP is able to control chain scission and to produce grafting in radiation-induced long-chain branching and crosslinking [9, 10]. The molecular structure of PP can be significantly modified by gamma radiation. The main molecular effects are chain scission, chain branching, and/or crosslinking [11, 12]. PP undergoes net crosslink, and significant levels of main-chain scission on irradiation, according to studies concerning the understanding of molecular weight change and the rate of gel formation under irradiation [13, 14]. According to Suljovrujic [15], degradation was the major reaction in the initial step of irradiation, independent of the atmosphere. The iPP irradiated in acetylene had the lowest values for oxidation level and $G(S)/G(X)$ values, in opposition of the highest values for air atmosphere. The results [15] confirm that oxidation strongly affects the gel point but has a much lower effect on the $G(S)/G(X)$ ratio. In the case of dielectric relaxation measurements, the connection between the oxidative degradation and dielectric properties is well established.

The PP grade having low melt flow index (MFI) values tends to have longer molecular chains and higher average molecular weight, which forms more molecular entanglements in the polymer melt. These polymers with a greater degree of molecular entanglements tend to have a higher resistance to extensional deformation yielding and higher melt strength [16].

Recent studies have investigated the deformation-induced changes in the structure of iPP films during uniaxial stretching at three different temperatures (room temperature, 60 and 160 °C) [17]. Another author has made this kind of experiment at 100 °C [25]. The chain entanglement in the interlamellar amorphous region plays an important role in the deformation-induced structure changes during uniaxial stretching. At low temperatures, as the chain mobility is relatively low, tie chains from entanglements may initiate the fragmentation of lamellar crystals upon stretching, forming an oriented mesomorphic iPP phase with extended-chain conformation. At high temperatures, as the chain mobility is relatively high, tensile

deformation can lead to chain disentanglement allowing the formation of more folded-chain crystals from coiled segments [17].

As part of an important study of the microstructure of iPP [18], the evolution during tensile deformation was examined by atomic force microscopy (AFM) and scanning electron microscopy (SEM), as a function of strain rate. Although both AFM and SEM are similar in lateral resolution, AFM has superior vertical resolution, and provides quantitative evaluation of surface topographical characteristics. The excellent resolution of AFM to describe surface topography has opened new opportunities to study surface deformation in polymeric materials [18–21]. Many authors have investigated the structure and morphological properties of stretched PP films [22, 23] and the influence of molecular orientation on the crosslinking behavior iPP, exposed to gamma radiation [24, 25].

The aim of this study is the investigation of the microstructure and morphology of the modified and original PP under stretching. Moreover, the measurements of differential scanning calorimetry (DSC) allowed the crystallinity evaluation.

Experimental

Materials and methods

The iPP with MFI = 1.5 dg min⁻¹, ASTM D 1238-4 [26] and Mw = 338,000 g mol⁻¹ from Braskem—Brazil, was supplied in pellets. The iPP pellets were conditioned in nylon bags and there fluxed several times with acetylene 99.8%, supplied by White Martins, under pressure of 110 kPa [9]. The irradiation process of the pellets placed in those bags was performed in a ⁶⁰Co gamma source at dose rate of 5 kGy h⁻¹. The radiation doses were 5, 12.5, and 20 kGy monitored by a Harwell Red Perspex 4034 dosimeter. After irradiation, the pellets were submitted to thermal treatment at 90 °C for 1 h to promote the recombination and annihilation of residual radicals [27]. The PP films were obtained by compression molding at 190 °C—10 min with no pressure and 5 min under a pressure of 80 bar—and dive into a water tank at 23 °C, which generally favors the formation of an amorphous phase.

Stress–strain

The samples were manufactured at dimensions according to ASTM D 882-09 [28]. The film stretching was performed at 170 °C in an Instron machine under a strain rate of 0.17 s⁻¹. Figure 1—where a refers to pristine and b to 12.5 kGy—shows the PP film stretched in an Instron machine at 170 °C.

Atomic force microscopy

The atomic force microscopy measurements were performed with a scanning probe microscope Nanoscope III A, made by Digital Instruments (Veeco) and equipped with multi-mode heads. The probe used for the images acquisition was commercial

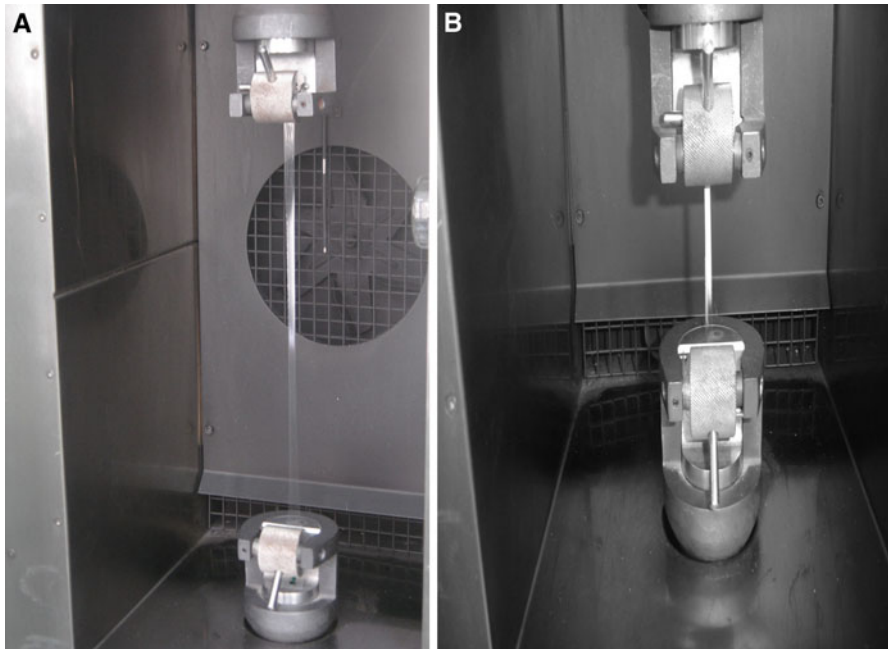


Fig. 1 a Pristine and b 12.5 kGy, Instron machine with film stretched

mode made of Si, with resonant frequency of about 250 kHz. The images were obtained using 512×512 pixels. Experiments were performed in tapping mode with an E scanner ($10 \times 10 \times 2.5$) μm^3 .

Scanning electron microscopy

Scanning electron microscopy was done using an EDAX PHILIPS XL 30. In this study, a thin coat of gold was sputter-coated onto the samples.

Thermal analysis

Thermal properties of specimens were analyzed using a differential scanning calorimeter (DSC) 822, Mettler Toledo. The thermal behavior of the films was obtained by: (1) heating from 25 to 280 °C at a heating rate of $10 \text{ }^\circ\text{C min}^{-1}$ under nitrogen atmosphere, (2) holding for 5 min at 280 °C, and (3) then cooling to 25 °C and reheating to 280 at $10 \text{ }^\circ\text{C min}^{-1}$, according to ASTM D 3418-08 [29]. The crystallinity was calculated according to the equation:

$$X_C(\%) = \frac{\Delta H_f \times 100}{\Delta H_0} \quad (1)$$

where ΔH_f is melting enthalpy of the sample, ΔH_0 is melting enthalpy of the 100% crystalline PP which is assumed to be 209 kJ kg^{-1} [7, 30].

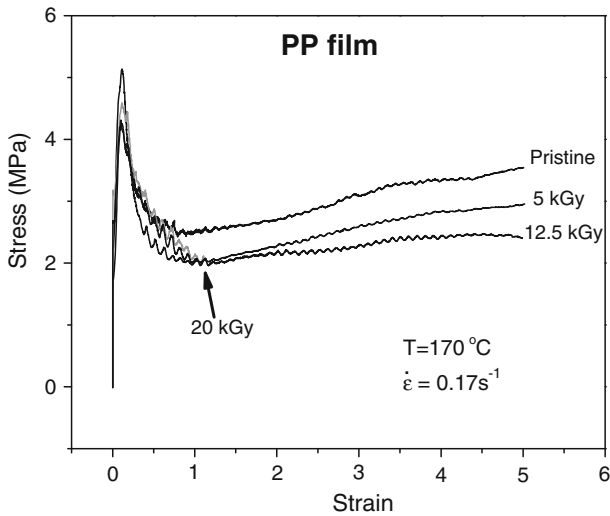


Fig. 2 Stress–strain curves for the PP film stretched up to rupture at 170 °C with a strain rate of 0.17 s⁻¹ ($l_0 = 50$ mm)

Results and discussion

Stress–strain

Figure 2 shows the stress–strain curves for the pristine and modified PP films.

The curves show the typical ductile deformation behavior, where a yield point is followed by a smooth strain hardening, well known for semi-crystalline polymers in tensile experiments, with the exception of the 20 kGy irradiated film that broke at strain equal to 1. In our case, it was assumed that the original PP crystals were melted as the stretching was performed at 170 °C, so we postulate that the yielding can be attributed to the new crystals induced by the elongational flow as a result of entanglements and/or crosslinkings of the polymer chains. However, at 170 °C there was a possibility of some remaining crystallinity, therefore the yield can also be caused by non melted crystals. The higher value to the pristine PP film was attributed to the greater molecular weight compared to the modified (irradiated) PP films that have been submitted to scission, branching and crosslinking. The lower yield stress for the 5 and 12.5 kGy irradiated films, compared to pristine, was a consequence of the prevalence of the chain scission over the branching and crosslinking at low doses [31]. For the 20 kGy sample, the yield stress increased and the elongation at rupture decreased due to the high level of crosslinking.

Atomic force microscopy

Figure 3 shows a representative image for the surface morphology of PP films, obtained by AFM.

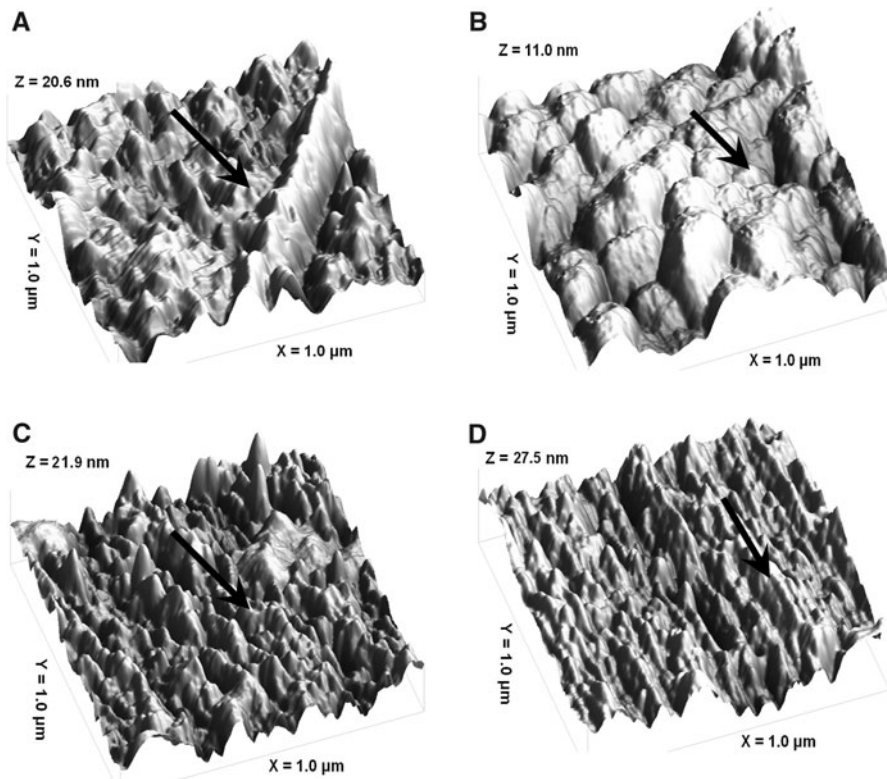


Fig. 3 Atomic force microscopy 3D images of pristine and irradiated stretched samples: **a** iPP Pristine, **b** PP 5 kGy, **c** PP 12.5 kGy, and **d** PP 20 kGy

The stretching direction is indicated by an arrow in Fig. 3. When PP film is stretched at 170 °C, a significant change in the surface of the material takes place. It is observed that the formation of microfibrillar structures of modified PP was aligned with the stretching direction.

Figure 4 shows some fibrils with an average diameter of 180 nm that are uniformly distributed on the surface of the 5 kGy sample. In this case, the number of fibrils by micrometer (approximately, 7) is the lower of the irradiated samples, which are 12 and 13, for 12.5 and 20 kGy samples, respectively.

Scanning electron microscopy

The SEM images showed the presence of molecular alignment in the same direction as the stretching, as indicated by the arrows in Fig. 5.

The fibrillar structure oriented along the stretching direction is the dominating morphological feature shown in the images in Fig. 5. This figure also presented surface regions with parallel microfibrils.

Fig. 4 Atomic force microscopy image for stretched sample PP 5 kGy

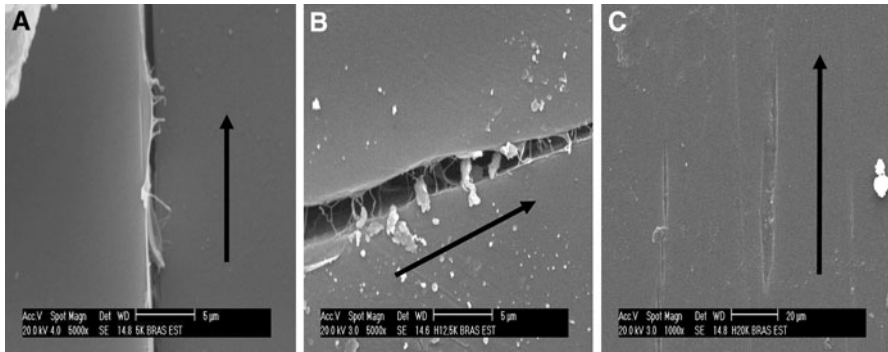
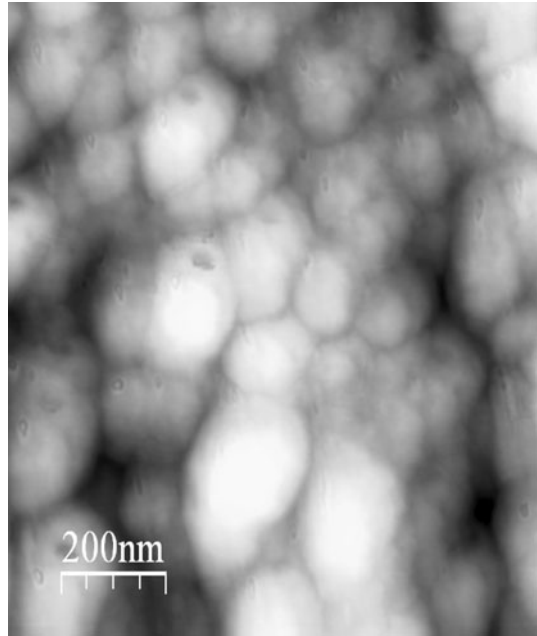


Fig. 5 **a** PP 5 kGy film, scale 5 μm, **b** PP 12.5 kGy film, scale 5 μm and **c** PP 20 kGy film, scale 20 μm

Table 1 Crystallinity (%) ($\pm 5\%$) and melting temperature ($^{\circ}\text{C}$) of (1 $^{\circ}$ event melt) of PP films before and after stretching

	Pristine PP		PP 5 kGy		PP 12.5 kGy		PP 20 kGy	
	χ_{c1} (%)	T_{m1} ($^{\circ}\text{C}$)	χ_{c1} (%)	T_{m1} ($^{\circ}\text{C}$)	χ_{c1} (%)	T_{m1} ($^{\circ}\text{C}$)	χ_{c1} (%)	T_{m1} ($^{\circ}\text{C}$)
Before stretching	33.3	165.0	35.3	164.6	39.9	164.6	33.8	161.3
After stretching	38.3	165.3	51.9	167.9	50.9	167.8	48.9	165.9

Thermal analysis

The level of crystallinity (%) was calculated according to Eq. 1 and melting temperatures were determined from the first melting event in the DSC. Table 1 summarizes the results of the pristine and modified (irradiated) films, before and after stretching.

The crystallinity increases after stretching as expected. On the stretched condition the irradiated films crystallinity was at around 30% higher than that of the pristine film. This difference is most probably due to the scission of soft segment chains that underwent stress-induced crystallization. Moreover, there was a contribution to the crystallinity from the creation of the fiber-like structure, due to the stretching process at high temperature. The lower irradiation doses also favor the crystallization and the improvement of fibril diameter (as shown in Fig. 4), due to the reduction of molecular size by chain scission mechanism, the only exception being the 20 kGy sample case, where crosslinking clearly dominated the overall process and with a lower crystallinity in both situations, before and after stretching.

The first DSC heating reveals an endothermic melting temperature of 165.0 and 165.3 °C for the non irradiated samples before and after stretching, respectively. The samples irradiated at 5 and 12.5 kGy showed a slight increase for melting temperatures before stretching and after stretching, 3.3 and 3.2 °C, respectively, whereas the melting temperature at the irradiation dose of 20 kGy shows a larger variation, 4.6 °C. As the film is stretched, these regions undergo substantial orientation and orientation-induced crystallization occurs. According to Koike and Cakmak [32], this process essentially is coupled with the partial break up and reorientation and recrystallization of some of the preexisting crystallites.

Conclusions

The stretching process at high temperature (170 °C) creates a micrometer-scale fiber-like network structure in the pristine iPP and irradiated iPP films. This structure consists of microfibrils parallel and perpendicular to the stretching direction. The predominant location of cracks between fibrils suggests that crack propagation is strongly dependent of fibril orientation.

The film irradiated with the higher dose, 20 kGy, presents coarse streaks which reveal the difficulty to align fibrils in the stretching direction. On a nanometer scale the entanglement involving crosslinked and/or branched chains in the amorphous phase is the primary cause for this phenomenon.

The increase in crystallinity of the irradiated and subsequently stretched films is due to the crystallization of the chain segments of the amorphous phase that suffered scission process as well as the crystallization of the tie chain.

Acknowledgments The authors wish to thank Conselho Nacional de Desenvolvimento Científico e Tecnológico (CNPq), Financiadora de Estudos e Projetos (FINEP proc.# 520015/2006-1), Centre of Science and Technology of Materials—CTM/IPEN for microscopy analysis (SEM), Laboratório de Filmes Finos do Instituto de Física da Universidade de São Paulo, for the SPM facility (FAPESP proc. #95/5651-0), Eleosmar Gasparin for DSC analysis and Companhia Brasileira de Esterilização (CBE) for irradiating the samples.

References

1. Borsig E, Duin M, Gotsis AD, Picchioni F (2008) Long chain branching on linear polypropylene by solid state reactions. *Eur Polym J* 44:200–212
2. Otaguro H, Artel BWH, Parra DF, Cardoso ECL, Lima LFCP, Lugao AB (2004) Polypropylene in the presence of trifunctional monomers and their influence in PP morphology. *Polimeros: Ciência e Tecnologia* 14(2):99–104
3. McCallum TJ, Kontopoulou M, Park CB, Muliawan EB, Hatzikiriakos SG (2007) The rheological and physical properties of linear and branched polypropylene blends. *Polym Eng Sci* 47(7): 1133–1140
4. Rätzsch M, Arnold M, Borsig E, Bucka H, Reichelt N (2002) Radical reactions on polypropylene in the solid state. *Prog Polym Sci* 27:1195–1282
5. Yoshiga A, Otaguro H, Lima LFCP, Artel BWH, Parra DF, Bueno JR, Shinzato R, Farrah M, Lugao AB (2007) Study of polypropylene/polybutene blends modified by gamma irradiation and (high melt strength polypropylene)/polybutene blends. *Nucl Instrum Methods Phys Res B* 265:130–134
6. Zhang XC, Butler MF, Cameron RE (1999) The relationships between morphology, irradiation and the ductile-brittle transition of isotactic polypropylene. *Polym Int* 48:1173–1178
7. Stojanovic Z, Kacarevic-Popovic Z, Galovic S, Milicevic D, Suljovrucic E (2005) Crystallinity changes and melting behavior of the uniaxially oriented iPP exposed to high doses of gamma radiation. *Polym Degrad Stab* 87:279–286
8. Abiona A, Osinkolu AG (2010) Gamma-irradiation induced property modification of polypropylene. *Int J Phys Sci* 5(7):960–967
9. Yoshiga A, Otaguro H, Parra DF, Lima LFCP, Lugao AB (2009) Controlled degradation and crosslinking of propylene induced by gamma radiation and acetylene. *Polym Bull* 63:397–409
10. Cheng S, Phillips E, Parks L (2010) Processability improvement of polyolefins through radiation-induced branching. *Radiat Phys chem* 79:329–334
11. Valenza V, Piccarolo S, Spadaro G (1999) Influence of morphology and chemical structure on the inverse response of polypropylene to gamma radiation under vacuum. *Polymer* 40:835–841
12. Otaguro H, Lima LFCP, Parra DF, Lugao AB, Chinelatto MA, Canevarolo SV (2010) High-energy radiation forming chain scission and branching in polypropylene. *Radiat Phys chem* 79:318–324
13. Hill T, Whittaker AK (2005) Encyclopedia of polymer science and technology. In: Radiation chemistry of polymers. Wiley, New York, pp 15–16
14. Spadaro G, Valenza A (2000) Calorimetric analysis of an isotactic polypropylene gamma-irradiated in vacuum. *J Therm Anal Calorim* 61:589–596
15. Suljovrucic E (2009) Gel production, oxidative degradation and dielectric properties of isotactic polypropylene irradiated under various atmospheres. *Polym Degrad Stab* 94:521–526
16. Muke S, Ivanov I, Kao N, Bhattacharya SN (2001) The melt extensibility of polypropylene. *Polym Int* 50:515–523
17. Zuo F, Keum JK, Chen X, Hsiao B, Chen H, Lai SY, Wevers R, Li J (2007) The role of interlamellar chain entanglement in deformation-induced structure changes during uniaxial stretching of isotactic polypropylene. *Polymer* 48:6867–6880
18. Dasari A, Rohrmann J, Misra RDK (2003) Microstructural aspects of surface deformation processes and fracture of tensile strained high isotactic polypropylene. *Mater Sci Eng A* 358:372–383
19. Dvir H, Jopp J, Gottlieb M (2006) Estimation of polymer-surface interfacial interaction strength by a contact AFM technique. *J Colloid Interface Sci* 304:58–66
20. Koike Y, Cakmak M (2006) The influence of molten fraction on the uniaxial deformation behavior of polypropylene: real time mechano-optical and atomic force microscopy observations. *J Polym Sci: Part B: Polym Phys* 44:925–941
21. Hoesier IL, Alamo RG, Lin JS (2004) Lamellar morphology of random metallocene propylene copolymers studied by atomic force microscopy. *Polymer* 45:3441–3455
22. Tabatabaei SH, Carreu PJ, Aji A (2009) Structure and properties of MDO stretched polypropylene. *Polymer* 50:3981–3989
23. Tabatabaei SH, Carreu PJ, Aji A (2009) Effect of processing on the crystalline orientation, morphology, and mechanical properties of polypropylene cast films and microporous membrane formation. *Polymer* 50:4228–4240
24. Oliani WL, Lima LFCP, Dias DB, Parra DF, Lugao AB (2010) Study of the morphology, thermal and mechanical properties of irradiated isotactic polypropylene films. *Radiat Phys Chem* 79:325–328

25. Suljovrujic E (2009) The influence of molecular orientation on the crosslinking/oxidative behaviour of iPP exposed to gamma radiation. *Eur Polym J* 45:2068–2078
26. ASTM D 1238-04—Standard test method for melt flow rates of thermoplastics by extrusion plastometer
27. Oliani WL, Parra DF, Lugao AB (2010) UV stability of HMSPP (high melt strength polypropylene) obtained by radiation process. *Radiat Phys Chem* 79:383–387
28. ASTM D 882-09—Standard test method for tensile properties of thin plastic sheeting
29. ASTM D 3418-08—Standard test method for transition temperatures and enthalpies of fusion and crystallization of polymers by differential scanning calorimetry
30. Brandrup J, Immergut EH, Grulke EA (1999) *Polymer handbook*, vol 1, 4th edn. Wiley Interscience, New York
31. Lugao AB, Noda L, Cardoso ECL, Hustzler B, Tokumoto S, Mendes ANF (2002) Temperature rising elution fractionation, infra red and rheology study on gamma irradiated HMSPP. *Radiat Phys Chem* 63:509–512
32. Koike Y, Cakmak M (2003) Real time development of structure in partially molten state stretching of PP as detected by spectral birefringence technique. *Polymer* 44:4249–4260